



Cite this: *Dalton Trans.*, 2024, **53**, 18013

The role of the stabilizing/leaving group in palladium catalysed cross-coupling reactions[†]

Lorenzo Palio, ^{‡,a,b} Francis Bru, ^{‡,a} Tommaso Ruggiero, ^a Laurens Bourda, ^a Kristof Van Hecke, ^a Catherine Cazin ^{*,a} and Steven P. Nolan ^{*,a}

Despite the widespread use of well-defined Pd^{II} complexes as pre-catalysts for cross-coupling processes, the role of the throw-away ligand is still underexplored. In this work we focused on the complexes of the type $[\text{Pd}(\text{NHC})(\eta^3\text{-R-allyl})\text{Cl}]$ (NHC = N-heterocyclic carbene) and we investigated the influence of the R substitution on the allyl moiety. Starting from the already described $[\text{Pd}(\text{IPr})(\eta^3\text{-cinnamyl})\text{Cl}]$ and $[\text{Pd}(\text{IPr}^*)(\eta^3\text{-cinnamyl})\text{Cl}]$ ($\text{IPr} = 1,3\text{-bis}(2,6\text{-diisopropylphenyl})\text{imidazol-2-ylidene}$, $\text{IPr}^* = N,N'\text{-1,3-bis}[2,6\text{-bis}(diphenylmethyl)-4-methylphenyl]\text{imidazol-2-ylidene}$) we prepared eight new complexes bearing new substitutions on the cinnamyl motif and we tested them in the C–N bond formation to evaluate the effect of the throw-away ligand modification in the catalytic activity. In addition, we studied the undesired formation of the less active off-cycle $[\text{Pd}_2^{\text{I}}(\text{NHC})_2(\eta^3\text{-R-allyl})(\mu\text{-Cl})]$ dimers from the corresponding Pd^{II} complexes to evaluate the role of the new throw-away ligands on the inhibition of this process.

Received 5th September 2024,
Accepted 14th October 2024

DOI: 10.1039/d4dt02533d

rsc.li/dalton

Introduction

Palladium N-heterocyclic carbenes (NHCs) have been widely studied in the last decades.^{1–5} They have been ubiquitously investigated for applications in homogeneous catalysis, especially in cross-coupling reactions.^{6–13} This class of organometallic compounds have the advantage to be air and moisture stable and permit a strict control on the metal-ligand stoichiometry, for which the ideal value has been proven to be 1 : 1.^{14,15} This well-defined approach to catalysis allows a deeper knowledge of the catalytic system and has been embraced by other research groups in recent years.^{16–19} The steric bulk around the Pd center given by the NHCs plays an important role in the reductive elimination and the transmetalation process, overall increasing the catalytic activity of the complex.^{15,20,21}

One aspect of the well-defined Pd–NHCs systems that deserves to be studied more thoroughly is the role of the “throw-away” ligands. These species are responsible for the stability of the well-defined systems by occupying the coordination sites ensuring a stable oxidation state. These ligands

are reported to disconnect from the complex during the activation process from the Pd^{II} to the Pd^0 active species.^{22,23} Therefore, the nature of the throw-away ligand plays a key role in the activity of the complex. One of the most widespread Pd–NHC pre-catalyst structures is the $[\text{Pd}(\text{NHC})(\eta^3\text{-R-allyl})\text{Cl}]$ type, developed for the first time by us in 2002, in which the allyl-based throw-away ligand ensures a fast and easy activation of the catalyst^{23–25} (Fig. 1).

Palladium(II) complexes of the type of $[\text{Pd}(\text{NHC})(\eta^3\text{-R-allyl})\text{Cl}]$ system (R = allyl, crotyl, cinnamyl, indenyl) have shown great activity for a wide range of C–C and C–heteroatom bond formation reactions.^{24–33} Particularly, the design of the allyl-modified moiety $[\text{Pd}(\text{NHC})(\eta^3\text{-cin})\text{Cl}]$ (cin = cinnamyl) complex class by 2006 was examined in order to achieve a faster activation to the $\text{Pd}(0)$ active species at lower temperatures.^{24,34,35} This latter generation of allyl systems was designed with the help of teaching from Trost and Tsuji on allylic alkylation and the relative stability/reactivity of substituted allyl fragments bound to Pd. Later, this was further elaborated by Colacot and Grasa at Johnson Matthey in their construction of Pd–allyl

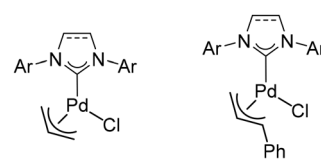
^aDepartment of Chemistry, Center for Sustainable Chemistry, Ghent University, Krijgslaan 281 (S-3), 9000 Ghent, Belgium

^bUniv. Lille, CNRS, Centrale Lille, ENSCL, Univ. Artois,

UMR 8181 – UCCS Unité de Catalyse et Chimie Solide, F-59000 Lille, France

[†]Electronic supplementary information (ESI) available: Experimental procedures, NMR spectra and XRD data. CCDC 2367688–2367692. For ESI and crystallographic data in CIF or other electronic format see DOI: <https://doi.org/10.1039/d4dt02533d>

[‡]These authors contributed equally to the work.



Nolan, 2002

Nolan, 2006

Fig. 1 Examples of well-defined Pd–NHC allyl-based complexes.



systems where the Buchwald ligands are the ancillary supporting ligands.¹⁶

Substitution at the allyl terminus leads to destabilisation of the allyl fragment bound to palladium and therefore to easier activation leading to the putative "Pd-NHC" species. This ease of activation in such systems, a pre-catalytic step whose importance is too often ignored, leads to Suzuki-Miyaura and the Buchwald-Hartwig cross-couplings involving unactivated aryl halides that can be performed at room temperature. The effect of bulky substituents on the other palladium ligand also profoundly affects catalytic activity. Indeed, systems bearing a bulky NHC such as in $[\text{Pd}(\text{IPr}^*)(\eta^3\text{-R-allyl})\text{Cl}]$ ($\text{IPr}^* = N,N'\text{-1,3-bis}[2,6\text{-bis}(\text{diphenylmethyl})\text{-4-methylphenyl}]$ imidazol-2-ylidene) and $[\text{Pd}(\text{anti-}(2,7)\text{-}(\text{SiCyOctNap}))(\eta^3\text{-cin})\text{Cl}]$ permit difficult cross-coupling reactions under very mild conditions. The typical example is their use in the formation of tetra-*ortho*-substituted biaryls.^{36,37} An interesting observation here is that crowded environments about the Pd pre-catalysts architecture allow for highly congested junctions in C-C and C-N bond making reactions to be formed.

Among the plethora of cross-coupling reactions, the Buchwald-Hartwig amination of aryl halides is one of the most widespread examples representing an efficient tool for the synthesis of several pharmaceutical agents.³⁸⁻⁴³ Several salient examples of the use of palladium N-heterocyclic carbene complexes in this C-N coupling exist in the literature.^{24,28,29,44-47}

Hazari and co-workers proposed the activation mechanism of the $[\text{Pd}(\text{NHC})(\eta^3\text{-R-allyl})\text{Cl}]$ species in presence of a weak base and suggested the presence of an equilibrium between the Pd^0 -NHC active species and the less active $[\text{Pd}_2^1(\text{NHC})_2(\mu\text{-}\eta^3\text{-R-allyl})(\mu\text{-Cl})]$ species^{48,49} (Fig. 2). In the report, it was shown that the presence of a R substituent on the allyl moiety raises the kinetic barrier of the comproportionating reaction between the Pd^{II} and the Pd^0 species, thereby increasing the concentration of the active monoligated species.⁴⁹

Results and discussion

Taking from these teachings, we have now prepared new substituted $[\text{Pd}(\text{NHC})(\eta^3\text{-R-allyl})\text{Cl}]$ complexes to explore their activity in the C-N bond formation. Efforts were also aimed at

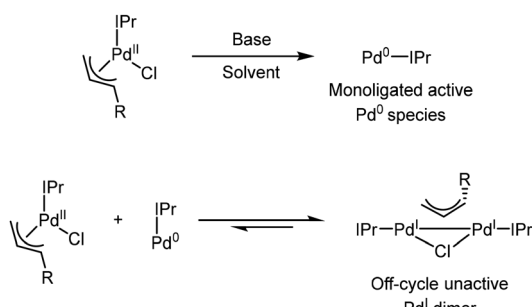


Fig. 2 Scheme of the activation and the dimerization via comproportionation presented by the Hazari group.⁴⁹

minimizing or entirely blocking the decomposition route that leads to inactive dimer formation. To achieve this, four new dimeric synthons were designed bearing bulkier allyl substituents and synthesised (Fig. 3). These were then converted to well-defined $[\text{Pd}(\text{NHC})(\eta^3\text{-R-allyl})\text{Cl}]$ complexes to further explore the role of the allyl throw-away ligand and its role in the decomposition route and define productive reactivity in a model palladium-mediated cross-coupling reaction.

Synthesis of $[\text{Pd}(\text{NHC})(\eta^3\text{-R-cin})\text{Cl}]$ complexes

The synthesis of the new complexes involves the cleavage of the novel $[\text{Pd}(\eta^3\text{-R-cin})(\mu\text{-Cl})_2]$ dimer (**1-4**) with the corresponding imidazolium salt in the presence of an excess of potassium carbonate in acetone at 60 °C for 5 h. The $[\text{Pd}(\eta^3\text{-R-allyl})(\mu\text{-Cl})_2]$ dimers were prepared starting from the corresponding allyl chloride following the reported procedure (Fig. 4).⁵⁰

The corresponding $[\text{Pd}(\text{NHC})(\eta^3\text{-R-allyl})\text{Cl}]$ complexes are obtained with good yields (>80%) using the weak base route.⁵¹ As an alternative synthetic route, the $[\text{Pd}(\text{NHC})(\eta^3\text{-R-allyl})\text{Cl}]$ complexes can be obtained through oxidative addition of the R-allyl chloride with our previously reported $[\text{Pd}(\text{NHC})(\text{PhC}\equiv\text{CPh})]$ synthon.⁵² This route allows rapid functionalization and derivatization from a common synthon, the $[\text{Pd}(\text{NHC})(\eta^3\text{-allyl})\text{Cl}]$. (See the Experimental section and ESI† for further details) (Fig. 5A and B).

Both palladium dimers and the $[\text{Pd}(\text{NHC})(\eta^3\text{-R-allyl})\text{Cl}]$ series are air- and moisture-stable and can be stored on a shelf in air for an indefinite amount of time. Single crystals for X-ray analysis were obtained for all the $[\text{Pd}(\eta^3\text{-R-allyl})(\mu\text{-Cl})_2]$ dimers by slow diffusion of hexane vapour into a saturated solution of the complex in dichloromethane.

Room temperature Buchwald–Hartwig amination of aryl chlorides

Reaction optimization. Next, the IPr and IPr* catalysts were deployed in the Buchwald–Hartwig reaction involving amines

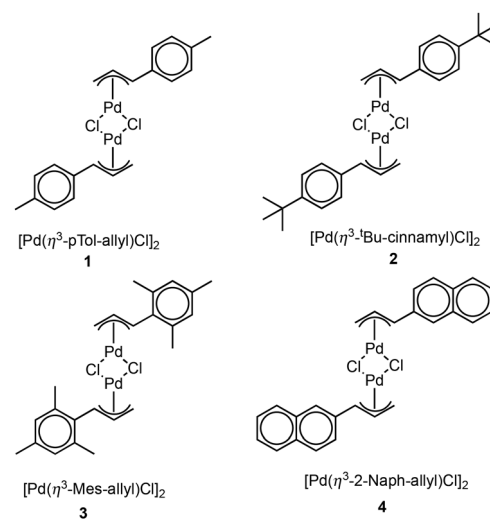


Fig. 3 Novel dimers (**1-4**) synthesized for this study.



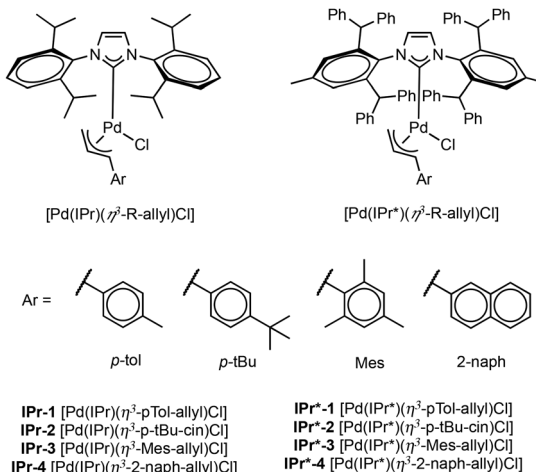


Fig. 4 Structures of the newly synthesised $[(\text{NHC})\text{Pd}(\eta^3\text{-R-allyl})\text{Cl}]$ pre-catalysts.

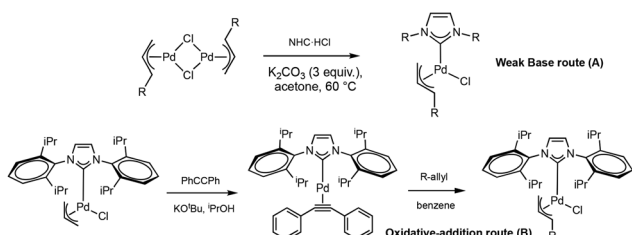


Fig. 5 The two possible synthetic routes leading to the novel pre-catalysts.

and aryl chlorides. The $[\text{Pd}(\text{NHC})(\eta^3\text{-cin})\text{Cl}]$ complexes have already been tested in this reaction. A series of allyl and cinnamyl Pd-NHC complexes have already been tested, showing the greater activity of the $[\text{Pd}(\text{SiPr})(\eta^3\text{-cin})\text{Cl}]$ in comparison to the IPr analogue,²⁴ and in general a significant improvement of the catalytic activity of the cinnamyl based species compared to the allyl analogues. After the development of the IPr* ligand, the $[\text{Pd}(\text{IPr}^*)(\eta^3\text{-cin})\text{Cl}]$ complex was tested in Buchwald–Hartwig amination as well.⁵³ All these examples showed great catalytic activity at room temperature with 1 mol% Pd loading and with dimethoxyethane (DME) as solvent in the presence of a strong base.^{24,53,54}

To compare the activity of the newly designed $[\text{Pd}(\text{NHC})(\eta^3\text{-R-allyl})\text{Cl}]$ complexes, these were tested under identical conditions as those already mentioned in the Buchwald–Hartwig amination, permitting an evaluation of the effect of the substitution on the phenyl ring of the cinnamyl moiety with both IPr and IPr* ligands. The reaction between morpholine and 2,6-dimethylchlorobenzene was chosen as a model reaction (Table 1). Initially, the four new $[\text{Pd}(\text{IPr})(\eta^3\text{-R-allyl})\text{Cl}]$ species were tested alongside the $[\text{Pd}(\text{IPr})(\eta^3\text{-cin})\text{Cl}]$ standard. The cross-coupling was performed at room temperature with 1 mol% of Pd and KO'Bu as base in anhydrous DME. The reaction with $[\text{Pd}(\text{IPr})(\eta^3\text{-cin})\text{Cl}]$ is reported to reach completion

Table 1 Screening of the catalysts in the cross-coupling reaction between morpholine and 2,6-dimethylchlorobenzene

Catalyst	Time [h]	Conversion ^a
$[\text{Pd}(\text{IPr})(\text{cin})\text{Cl}]$	0.5/2.5	21/100
IPr-1	0.5/2/2.5	20/81/100
IPr-2	0.5/2/2.5	11/65/84
IPr-3	0.5/2/2.5	38/100/100
IPr-4	0.5/2/2.5	42/85/100
$[\text{Pd}(\text{IPr}^*)(\text{cin})\text{Cl}]$	0.5/2	55/92
IPr*-1	0.5/2	21/78
IPr*-2	0.5/2	37/75
IPr*-3	0.5/2	87/100
IPr*-4	0.5/2	65/97

Conditions: aryl chloride (0.5 mmol, 1 eq.), morpholine (0.55 mmol, 1.1 eq.), 0.5 mL of DME, reaction under inert atmosphere. ^a Average result of two separate experiments.

after 2 hours.²⁴ Complete conversion was reached by all catalysts after 2.5 h, with the only exception of **IPr-2** for which the conversion stopped at 84%, showing the lowest activity compared to the others. The conversion was also monitored after 30 minutes to evaluate the difference in activity. After this time, the aryl chloride conversion ratio was 21% when $[\text{Pd}(\text{IPr})(\eta^3\text{-cin})\text{Cl}]$ was used. A similar value of 20% was obtained with **IPr-1**, while **IPr-2** gave only 11% confirming the previous observation. **IPr-3** and **IPr-4** showed to be more active, giving respectively 42% and 38% conversions after 30 minutes. After 2 hours, **IPr-3** is the only species that gave 100% conversion of the starting material, while **IPr-4** reached 85%. **IPr-1** and **IPr-2** showed 81% and 65% conversion of the aryl chloride, following the trend previously observed. From these initial results, the substitution at the C4 of the phenyl ring of the cinnamyl moiety does not appear to improve catalyst activity, but rather leads to lower conversions. However, the modification on the *ortho* positions of the cinnamyl moiety, oriented towards the Pd center, leads to improved catalytic activity.

We next move to the more sterically congested IPr* analogues in the same cross-coupling reaction under identical conditions. The already described $[\text{Pd}(\text{IPr}^*)(\eta^3\text{-cin})\text{Cl}]$ structure bearing the unmodified cinnamyl group was used as standard. As in the previous case, all species reached full conversion after 2.5 hours.

After 30 minutes, **IPr*-3** showed the highest conversion value with 87%, followed by **IPr*-4** (65%), and by $[\text{Pd}(\text{IPr}^*)(\text{cin})\text{Cl}]$ (55%). On the other hand, **IPr*-1** and **IPr*-2** gave respectively 21% and 37% conversions. These conversion values achieved with the bulkier IPr* series are generally higher than the ones obtained with the IPr series, and concomitantly follow the same activity trend as a function of the cinnamyl substitution pattern. The substitution of the phenyl group with the mesityl showed the greatest increase in catalytic performance. The 2-naphthyl modification also leads to a higher

catalytic activity in comparison with the unsubstituted cinnamyl analogue. On the other hand, the **IPr^{*}-1** and **IPr^{*}-2** pre-catalysts that only bear substitution at the C4 of the cinnamyl moiety, showed a greater decrease in the conversion than the ones observed for the **IPr** series. After 2 hours, **IPr^{*}-3** converted 100% of the starting material, confirming it is the best pre-catalyst overall, while **IPr^{*}-4** provided almost full conversion at 97%, proving a greater activity than $[\text{Pd}(\text{IPr}^*)(\eta^3\text{-cin})\text{Cl}]$ that reached a 92% conversion. **IPr^{*}-1** and **IPr^{*}-2** converted respectively 80% and 75% of the starting material in 2 hours.

So, the steric congestion about the palladium center can be appreciated, single crystals of **IPr^{*}-3** were grown for diffraction studies. A graphical representation of the structure of **IPr^{*}-3** is presented in Fig. 6. It is clear from the metrical parameters that there exists a significant elongation of the Pd–C allyl bond when this carbon is substituted with a mesityl group ($\text{C}^{\text{allyl}3}$), going from 2.104(2) Å at the unsubstituted allylic terminus to the central allyl carbon (2.159(4) Å) to the mesityl bearing allylic terminus 2.305(4) Å. This compares to values of 2.110(7) Å, 2.270(10) Å and 2.155(11) Å for these three positions found for the related $[\text{Pd}(\text{IPr}^*)(\text{cin})\text{Cl}]$ complex (Table 2).³⁷ The substitution on the aryl fragment of the allyl evidently causes a major distortion of the allyl fragment effectively creating significantly more access to the palladium center in **IPr^{*}-3**.

Scope of the Buchwald–Hartwig amination reaction. A small array of aryl chlorides and amines was explored in the Buchwald–Hartwig amination using the most active **IPr^{*}-3** (Fig. 7). Morpholine reacted smoothly with chlorobenzene, 4-chlorotoluene and 4-chloroanisole affording **5a**, **5b** and **5c** in

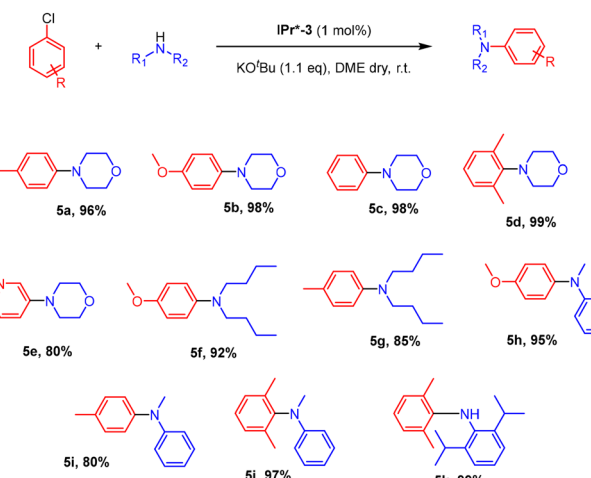


Fig. 7 Scope of the Buchwald–Hartwig reaction mediated by **IPr^{*}-3**. Isolated yields reported as an average of two separate experiments.

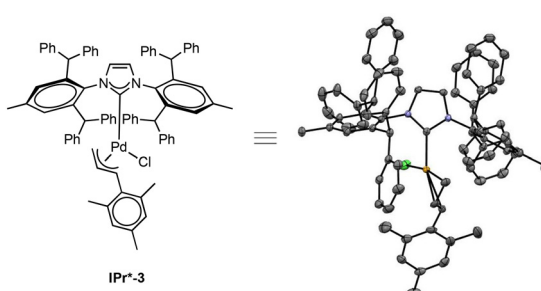


Fig. 6 X-ray structure of the **IPr^{*}-3** pre-catalysts showing the thermal displacement ellipsoids at 50% probability level. Hydrogen atoms are omitted for clarity. Selected bond distances (Å) and angles (°): Pd–Cl 2.3605(6), Pd–C^{NHC} 2.032(2), Pd–C^{allyl1} 2.104(2), Pd–C^{allyl2} 2.159(4), Pd–C^{allyl3} 2.305(4); C^{NHC}–Pd–Cl 92.46(6), C^{NHC}–Pd–C^{allyl1} 100.74(9), C^{allyl1}–Pd–C^{allyl3} 67.14(11), C^{allyl3}–Pd–Cl 99.98(9).

Table 2 Selected bond distances of **IPr^{*}-3** and $[\text{Pd}(\text{IPr}^*)(\text{cin})\text{Cl}]$

	Å	IPr[*]-3	$[\text{Pd}(\text{IPr}^*)(\text{cin})\text{Cl}]$
	Pd–C1	2.104(2)	2.110(7)
	Pd–C2	2.159(4)	2.270(10)
	Pd–C3	2.305(4)	2.155(11)

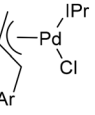
excellent yield. A lower yield was obtained when morpholine is coupled with 3-chloro pyridine, giving **5e** in 80% yield. Overall, the 4-chloroanisole seems interestingly more compatible with the system, since the reaction with sterically hindered and less reactive dibutyl amine provided **5f** in 92% yield, while the coupling of the same amine with the 4-chlorotoluene gave **5g** in an 85% yield. The reactions with methyl aniline followed the same trend as the previous examples, giving better results when 4-chloroanisole is employed in comparison to 4-chlorotoluene, giving respectively 95% and 80% yield (**5h** and **5i**). The system showed to be extremely effective with sterically hindered substrates. The di-*ortho* substituted 2,6-dimethylphenyl chloride was the most reactive among all substrates tested with morpholine and afforded **5d** in quantitative yield. The same aryl chloride reacted smoothly with methyl aniline giving **5j** in 97% yield. Furthermore, we noticed that when both the substrates are sterically demanding, the coupling occurs very smoothly, as in the case of the reaction of 2,6-dimethyl phenyl chloride with 2,6-diisopropyl aniline that provided the corresponding tetra-*ortho* diaryl amine **5k** in quantitative yield. This result highlights the high activity of **IPr^{*}-3** as these substrates usually require harsher conditions to proceed.⁵⁵

A factor that can be responsible for the increase in the catalytic activity of our new systems is the diminution of the formation of the off-cycle and catalytically inactive $[\text{Pd}^{\text{I}}(\text{NHC})_2(\eta^3\text{-R-allyl})(\mu\text{-Cl})]$ species. The preparation of these dimers can be achieved by the reaction of the $[\text{Pd}(\text{NHC})(\eta^3\text{-R-allyl})\text{Cl}]$ complex with an excess of potassium carbonate in degassed EtOH under inert atmosphere.⁵⁶ Different Pd^I dimers bearing various NHCs are reported within a maximum time of 5 hours. In this work, we aimed to investigate the ease of formation of the Pd^I dimers starting from the new $[\text{Pd}(\text{NHC})(\eta^3\text{-R-allyl})\text{Cl}]$ pre-catalysts.

Initially, the four IPr-bearing palladium complexes were investigated. The corresponding $[\text{Pd}(\text{NHC})(\eta^3\text{-R-allyl})\text{Cl}]$ complex was reacted with 3 eq. of K_2CO_3 in EtOH and the ratio



Table 3 Decomposition and formation times for the Pd^{I} dimers preparation

	Complete decomposition time (h)	Pd^{I} dimer formation starting time	Acetaldehyde formation starting time (h)
IPr-1	1	2	4
IPr-2	1	1	2
IPr-3	1	1	1
IPr-4	2	1	1

between the formed dimer and the remaining Pd^{II} complex was evaluated every hour for 5 hours.

The central proton peak of the allyl system is reported to be abnormally shifted upfield, around 1.70 ppm (ref. 49) due to the high electronic density present on the allyl fragment caused by the back-bonding from the d orbitals of the Pd–Pd bonding to the π^* orbital of the allyl moiety.^{49,57,58} Therefore, the signal of this central proton was selected to monitor dimer formation. For **IPr-1**, already after 1 h of reaction, a sharp decrease of the signals of the allyl system of the monomeric species was observed, along with the appearance of a peak around 1.85 ppm. The signal of acetaldehyde, formed from the oxidation of ethanol, is detected starting from 4 h. From the reaction involving **IPr-2**, the complete decomposition of the monomeric complex occurs already after 1 h. Many species that are difficult to detect are formed during the experiment, the Pd^{I} dimer appears after 1 h, but decomposes during the time. The aldehydic proton of the acetaldehyde and the olefin signal of the species that is formed in the reductive elimination step that leads to the monoligated Pd^0 species disconnected from the Pd are also noticeable (see the ESI† for further details). For **IPr-3**, after 1 h, no Pd^{II} precursor remains. On the other hand, significant amounts of acetaldehyde were detected during the 5-hour reaction time starting already after 1 h. This result suggests that this catalyst is easily activated, forming the monoligated L-Pd⁰ fragment, but has less of a tendency to form the Pd^{I} dimer due to the steric hindrance of the mesityl group on the allyl moiety. The experiment with **IPr-4** is the only one that shows that after 1 h the precursor is still not completely decomposed, suggesting a slower Pd^{I} dimer formation for this species. A summary of these results is reported in Table 3. On the other hand, the IPr* complexes did not show any Pd^{I} dimer formation. This we suspect is due to the significant steric hindrance of the IPr* ligand.⁵⁶

Experimental

Synthetic procedures

General procedure for synthesis of the allyl chlorides. A modified literature procedure is used for the synthesis of the allyl chlorides:⁵⁹ R-benzaldehyde was charged to a nitrogen filled round-bottom flask filled with nitrogen and dissolved in dry THF. This mixture was cooled to 0 °C and 1.2 equiv. of

vinylmagnesium bromide (1.0 M in THF) was added. The mixture was then allowed to warm to room temperature and was stirred for 2 hours. After completion (determined by TLC), the reaction is quenched with a saturated solution of NH_4Cl in water and extracted three times with ethyl acetate. The combined organic phases were collected and concentrated using a rotary evaporator. This crude alcohol is directly used in the next step. The alcohol of the previous step is dissolved in dry dichloromethane under a nitrogen atmosphere and cooled to 0 °C. 4 equivalents of SOCl_2 are added and the mixture is stirred for 2 hours at 0 °C. Afterwards, the mixture is allowed to warm to room temperature and stirred for an additional hour. After completion (determined using TLC), the reaction is quenched with ice water and extracted three times with dichloromethane. The combined organic phases are dried using Na_2SO_4 , filtered and concentrated *in vacuo*. The crude is then further purified using vacuum distillation or recrystallisation. Identity of the product is confirmed by comparing ¹H-NMR to literature values.^{59–62}

General procedure for synthesis of $[\text{Pd}(\eta^3\text{-R-allyl})(\mu\text{-Cl})_2]$. In a round bottom flask, PdCl_2 (1 equiv.) and NaCl (2 equiv.) are dissolved in 5 mL of warm water (30 °C) and stirred for 15 min. After this time, R-allyl (1 equiv.) dissolved in 10 mL of methanol is added to the reaction. Additional methanol is added to ensure homogeneity. The flask is sealed with a rubber septum and a balloon filled with CO, fitted onto a needle, is used to bubble gas through the solution. After two hours, the solution had turned from red brown to yellow. Sometimes, Pd-black formed, completely taking over the colour of the solution, this however can be removed during work-up. The reaction is stopped, and the solution is poured into a separation funnel containing 50 mL water. The mixture is extracted with chloroform (3 × 30 mL). The collected organic phases are dried using MgSO_4 and the mixture is filtered through a frit resulting in a clear yellow solution. The solvent is evaporated *in vacuo* to concentrate the solution. Hexane is added as a co-solvent and after sonication and filtration the product is collected on a frit, washed with cold hexane, and dried *in vacuo*.

General procedure for the synthesis of $[\text{Pd}(\text{NHC})(\eta^3\text{-R-allyl})\text{Cl}]$ via the weak-base route. A 4 mL vial, is charged with $[\text{Pd}(\eta^3\text{-R-allyl})(\mu\text{-Cl})_2$] (1 equiv.), $\text{NHC}\cdot\text{HCl}$ (2.4 equiv.), K_2CO_3 (3 equiv.) and 2 mL of acetone are added. This mixture is heated to 60 °C and stirred vigorously for 5 hours. After this reaction time, the solvent is evaporated *in vacuo* and the remaining solid residue is dissolved in DCM. This solution is filtered over a Florisil® plug and washed with more DCM. The filtrate is then concentrated *in vacuo* to remove volatiles. Pentane is added to the concentrate solution to assist the precipitation of the complex with the aid of a sonication bath. The solution is filtered affording the desired product as a solid.

General procedure for synthesis of $[\text{Pd}(\text{NHC})(\eta^3\text{-R-allyl})\text{Cl}]$ via Pd^0 -synthon route. In the glovebox: a 4 mL vial is charged with $[\text{Pd}(\text{IPr})(\text{PhC}\equiv\text{CPh})]$ ⁵² (1 equiv.) and benzene. This mixture is stirred at room temperature for 15 minutes after



which time the vial is removed from the glovebox for the work-up. The solvent is evaporated *in vacuo* and the remaining solid is dissolved in a minimal amount of DCM. The desired product is then recrystallised by adding pentane and sonication, and isolated by filtration and washed with cold pentane.

[Pd₂(NHC)₂(η³-R-allyl)(μ-Cl)] dimer formation. [Pd(NHC)(η³-R-allyl)Cl] (0.08 mmol, 1 eq.), K₂CO₃ (0.24 mmol), and a magnetic stirring bar were charged into a Schlenk flask, followed by 3 vacuum/argon cycles and then the degassed ethanol (3 mL) was transferred into the flask. The reaction mixture was stirred at 40 °C for 24 h. A sample of 0.1 mL was taken and added to an NMR tube. The solvent was evaporated and CDCl₃ was added. The samples were analyzed by ¹H NMR every hour until 5 h to monitor the reaction progress.

Crystallography. The single crystals of the dimers (**1–4**) and of **IPr^{*}-3** for XRD analysis were grown by dissolving 0.5 mg of the complex in 1 mL of DCM and subsequent slow diffusion of hexane at 4 °C. Deposition number CCDC 2367688–2367692† (for **1**, **2**, **3**, **4** and **IPr^{*}-3**) contain the supplementary crystallographic data for this paper.

Conclusions

We have successfully prepared a new series of [Pd(NHC)(η³-R-allyl)Cl] complexes bearing a substituted-cinnamyl moiety, with the metal center decorated with IPr or IPr^{*} ligands. The influence of the bulkier throw-away ligands was studied by testing the pre-catalysts in the Buchwald–Hartwig cross-coupling reaction. The results showed that the naphthyl and the mesityl modifications on the allyl motif led to an increase in catalytic activity when compared to the unsubstituted cinnamyl-based complexes. On the other hand, the substitution with *p*-tol and especially with the *p*-^tBu-phenyl groups resulted in a decrease in catalytic activity. This reactivity difference is significantly more pronounced when the NHC is IPr^{*}. The best catalyst among the series examined is [Pd(IPr^{*})(η³-mes-allyl)Cl] (**IPr^{*}-3**). The results highlight how this composition is particularly active for the preparation of bulky secondary and tertiary amines with 2,6-di-*ortho*-substituted starting materials. The higher reactivity is due to the complex stability, and this has been probed by attempting to transform the [Pd(NHC)(η³-R-allyl)Cl] complexes into catalytically inactive Pd(i) dimers. For the IPr-containing series this transformation clearly occurs under the specific reaction conditions examined. As for the IPr^{*} analogue, a complete lack of reactivity in this manner is observed. In this sterically more demanding series, the Pd(i) dimer formation is completely inhibited.

The series of experiments performed here on both modifying the allyl and NHC moieties teach us that to target a very active, yet stable pre-catalyst, one needs steric protection on the NHC hemisphere of the complex while also having a high degree of substitution on the allyl which serves two purposes: (1) it destabilises the Pd-allyl bond as it is highly substituted and (2) it hinders the role of the liberated allyl to act as a brid-

ging ligand in comproportionation reactions to stabilise the Pd(i) dimer structure. More work along these lines is presently ongoing in our laboratories.

Author contributions

LP and FB performed experimental work, contributed to writing the manuscript draft. TR, LB and KVH performed diffraction work. CC and SPN directed the work, contributed to the writing of the draft and final manuscript as well as secured funding.

Data availability

All data included and leading to conclusions presented in this manuscript are included in the ESI.†

Conflicts of interest

There are no conflicts to declare.

Acknowledgements

The Research Foundation – Flanders (FWO) (G0A6823N to SPN and G0C5423N to CSJC and G0A8723N to KVH) for financial support. Umicore AG are gratefully thanked for gifts of materials.

References

- 1 N. Marion and S. P. Nolan, *Acc. Chem. Res.*, 2008, **41**, 1440–1449.
- 2 S. Würz and F. Glorius, *Acc. Chem. Res.*, 2008, **41**, 1523–1533.
- 3 G. C. Fortman and S. P. Nolan, *Chem. Soc. Rev.*, 2011, **40**, 5151.
- 4 C. Valente, S. Çalimsiz, K. H. Hoi, D. Mallik, M. Sayah and M. G. Organ, *Angew. Chem., Int. Ed.*, 2012, **51**, 3314–3332.
- 5 R. D. J. Froese, C. Lombardi, M. Pompeo, R. P. Rucker and M. G. Organ, *Acc. Chem. Res.*, 2017, **50**, 2244–2253.
- 6 M. S. Viciu, R. A. Kelly, E. D. Stevens, F. Naud, M. Studer and S. P. Nolan, *Org. Lett.*, 2003, **5**, 1479–1482.
- 7 P. Lei, G. Meng, Y. Ling, J. An and M. Szostak, *J. Org. Chem.*, 2017, **82**, 6638–6646.
- 8 S. Shi and M. Szostak, *Chem. Commun.*, 2017, **53**, 10584–10587.
- 9 C. M. Zinser, F. Nahra, M. Brill, R. E. Meadows, D. B. Cordes, A. M. Z. Slawin, S. P. Nolan and C. S. J. Cazin, *Chem. Commun.*, 2017, **53**, 7990–7993.
- 10 S. Shi, S. P. Nolan and M. Szostak, *Acc. Chem. Res.*, 2018, **51**, 2589–2599.

11 S. Ostrowska, T. Scattolin and S. P. Nolan, *Chem. Commun.*, 2021, **57**, 4354–4375.

12 K. Wang, R. Fan, X. Wei and W. Fang, *Green Synth. Catal.*, 2022, **3**, 327–338.

13 S. Ostrowska, L. Palio, A. Czapik, S. Bhandary, M. Kwit, K. Van Hecke and S. P. Nolan, *Catalysts*, 2023, **13**, 559.

14 G. A. Grasa, M. S. Viciu, J. Huang and S. P. Nolan, *J. Org. Chem.*, 2001, **66**, 7729–7737.

15 H. Li, C. C. C. Johansson Seechurn and T. J. Colacot, *ACS Catal.*, 2012, **2**, 1147–1164.

16 L. L. Hill, J. L. Crowell, S. L. Tutwiler, N. L. Massie, C. C. Hines, S. T. Griffin, R. D. Rogers, K. H. Shaughnessy, G. A. Grasa, C. C. C. Johansson Seechurn, H. Li, T. J. Colacot, J. Chou and C. J. Woltermann, *J. Org. Chem.*, 2010, **75**, 6477–6488.

17 C. C. C. Johansson Seechurn, S. L. Parisel and T. J. Colacot, *J. Org. Chem.*, 2011, **76**, 7918–7932.

18 N. C. Bruno, M. T. Tudge and S. L. Buchwald, *Chem. Sci.*, 2013, **4**, 916–920.

19 N. C. Bruno, N. Niljianskul and S. L. Buchwald, *J. Org. Chem.*, 2014, **79**, 4161–4166.

20 G. Bastug and S. P. Nolan, *Organometallics*, 2014, **33**, 1253–1258.

21 X. Tian, J. Lin, S. Zou, J. Lv, Q. Huang, J. Zhu, S. Huang and Q. Wang, *J. Organomet. Chem.*, 2018, **861**, 125–130.

22 U. Christmann and R. Vilar, *Angew. Chem., Int. Ed.*, 2005, **44**, 366–374.

23 N. Hazari, P. R. Melvin and M. M. Beromi, *Nat. Rev. Chem.*, 2017, **1**, 0025.

24 N. Marion, O. Navarro, J. Mei, E. D. Stevens, N. M. Scott and S. P. Nolan, *J. Am. Chem. Soc.*, 2006, **128**, 4101–4111.

25 M. S. Viciu, R. F. Germaneau and S. P. Nolan, *Org. Lett.*, 2002, **4**, 4053–4056.

26 M. S. Viciu, R. F. Germaneau, O. Navarro-Fernandez, E. D. Stevens and S. P. Nolan, *Organometallics*, 2002, **21**, 5470–5472.

27 M. S. Viciu, O. Navarro, R. F. Germaneau, R. A. Kelly, W. Sommer, N. Marion, E. D. Stevens, L. Cavallo and S. P. Nolan, *Organometallics*, 2004, **23**, 1629–1635.

28 M. J. Cawley, F. G. N. Cloke, R. J. Fitzmaurice, S. E. Pearson, J. S. Scott and S. Caddick, *Org. Biomol. Chem.*, 2008, **6**, 2820–2825.

29 A. Chartoire, A. Boreux, A. R. Martin and S. P. Nolan, *RSC Adv.*, 2013, **3**, 3840–3843.

30 P. R. Melvin, A. Nova, D. Balcells, W. Dai, N. Hazari, D. P. Hruszkewycz, H. P. Shah and M. T. Tudge, *ACS Catal.*, 2015, **5**, 3680–3688.

31 P. R. Melvin, N. Hazari, H. M. C. Lant, I. L. Peczak and H. P. Shah, *Beilstein J. Org. Chem.*, 2015, **11**, 2476–2486.

32 C. M. Zinser, K. G. Warren, R. E. Meadows, F. Nahra, A. M. Al-Majid, A. Barakat, M. S. Islam, S. P. Nolan and C. S. J. Cazin, *Green Chem.*, 2018, **20**, 3246–3252.

33 Y. Liu, T. Scattolin, A. Gobbo, M. Beliš, K. Van Hecke, S. P. Nolan and C. S. J. Cazin, *Eur. J. Inorg. Chem.*, 2022, **2022**, e202100840.

34 P. Lei, G. Meng, Y. Ling, J. An, S. P. Nolan and M. Szostak, *Org. Lett.*, 2017, **19**, 6510–6513.

35 G. Li, P. Lei, M. Szostak, E. Casals-Cruañas, A. Poater, L. Cavallo and S. P. Nolan, *ChemCatChem*, 2018, **10**, 3096–3106.

36 L. Wu, E. Drinkel, F. Gaggia, S. Capolicchio, A. Linden, L. Falivene, L. Cavallo and R. Dorta, *Chem. – Eur. J.*, 2011, **17**, 12886–12890.

37 A. Chartoire, M. Lesieur, L. Falivene, A. M. Z. Slawin, L. Cavallo, C. S. J. Cazin and S. P. Nolan, *Chem. – Eur. J.*, 2012, **18**, 4517–4521.

38 B. Schlummer and U. Scholz, *Adv. Synth. Catal.*, 2004, **346**, 1599–1626.

39 J.-P. Corbet and G. Mignani, *Chem. Rev.*, 2006, **106**, 2651–2710.

40 C. Torborg and M. Beller, *Adv. Synth. Catal.*, 2009, **351**, 3027–3043.

41 M. M. Heravi, Z. Kheilkordi, V. Zadsirjan, M. Heydari and M. Malmir, *J. Organomet. Chem.*, 2018, **861**, 17–104.

42 P. A. Forero-Cortés and A. M. Haydl, *Org. Process Res. Dev.*, 2019, **23**, 1478–1483.

43 R. Emadi, A. Bahrami Nekoo, F. Molaverdi, Z. Khorsandi, R. Sheibani and H. Sadeghi-Aliabadi, *RSC Adv.*, 2023, **13**, 18715–18733.

44 G. Le Duc, S. Meiries and S. P. Nolan, *Organometallics*, 2013, **32**, 7547–7551.

45 S. Meiries, G. Le Duc, A. Chartoire, A. Collado, K. Speck, K. S. A. Arachchige, A. M. Z. Slawin and S. P. Nolan, *Chem. – Eur. J.*, 2013, **19**, 17358–17368.

46 Y.-C. Hsu and M.-T. Chen, *Eur. J. Inorg. Chem.*, 2022, **2022**, e202100828.

47 D.-Z. Zheng, H.-G. Xiong, A.-X. Song, H.-G. Yao and C. Xu, *Org. Biomol. Chem.*, 2022, **20**, 2096–2101.

48 P. R. Melvin, D. Balcells, N. Hazari and A. Nova, *ACS Catal.*, 2015, **5**, 5596–5606.

49 D. P. Hruszkewycz, D. Balcells, L. M. Guard, N. Hazari and M. Tilset, *J. Am. Chem. Soc.*, 2014, **136**, 7300–7316.

50 Y. Tatsuno, T. Yoshida, S. Otsuka, N. Al-Salem and B. L. Shaw, *Inorg. Synth.*, 1990, 342–345.

51 E. A. Martynova, N. V. Tzouras, G. Pisanò, C. S. J. Cazin and S. P. Nolan, *Chem. Commun.*, 2021, **57**, 3836–3856.

52 F. Bru, M. Lesieur, A. Poater, A. M. Z. Slawin, L. Cavallo and C. S. J. Cazin, *Chem. – Eur. J.*, 2022, **28**, e202201917.

53 M. S. Viciu, R. M. Kissling, E. D. Stevens and S. P. Nolan, *Org. Lett.*, 2002, **4**, 2229–2231.

54 A. Chartoire, X. Frogneux and S. P. Nolan, *Adv. Synth. Catal.*, 2012, **354**, 1897–1901.

55 Y. N. Timsina, G. Xu and T. J. Colacot, *ACS Catal.*, 2023, **13**, 8106–8118.

56 Y. Liu, V. A. Voloshkin, T. Scattolin, L. Cavallo, B. Dereli, C. S. J. Cazin and S. P. Nolan, *Dalton Trans.*, 2021, **50**, 5420–5427.

57 S. Sakaki, K. Takeuchi, M. Sugimoto and H. Kurosawa, *Organometallics*, 1997, **16**, 2995–3003.

58 H. Kurosawa, *Pure Appl. Chem.*, 1998, **70**, 1105–1110.



59 W.-F. Wang, J.-B. Peng, X. Qi, J. Ying and X.-F. Wu, *Chem. – Eur. J.*, 2019, **25**, 3521–3524.

60 W. Lölsberg, S. Ye and H.-G. Schmalz, *Adv. Synth. Catal.*, 2010, **352**, 2023–2031.

61 N. W. J. Ang, J. C. A. Oliveira and L. Ackermann, *Angew. Chem., Int. Ed.*, 2020, **59**, 12842–12847.

62 C. I. Jette, Z. J. Tong, R. G. Hadt and B. M. Stoltz, *Angew. Chem., Int. Ed.*, 2020, **59**, 2033–2038.

